

# On Causality in Dynamical Systems

Daniel Harnack\* and Klaus Richard Pawelzik†  
*University of Bremen, Institute for Theoretical Physics and  
 Center for Cognitive Science (ZKW)*  
 (Dated: August 1, 2018)

Identification of causal links is fundamental for the analysis of complex systems. In dynamical systems, however, nonlinear interactions may hamper separability of subsystems which poses a challenge for attempts to determine the directions and strengths of their mutual influences. We found that asymmetric causal influences between parts of a dynamical system lead to characteristic distortions in the mappings between the attractor manifolds reconstructed from respective local observables. These distortions can be measured in a model-free, data-driven manner. This approach extends basic intuitions about cause-effect relations to deterministic dynamical systems and suggests a mathematically well defined explanation of results obtained from previous methods based on state space reconstruction.

Keywords: Causality | Dynamical Systems | Topology | State Space Reconstruction

## INTRODUCTION

Causality has no universally accepted definition. For a dynamical system consisting of mutually coupled parts the notion of causality is particularly problematic since in general the dynamics of the overall system cannot be decomposed into components but rather behave as a whole. This fact becomes particularly evident from Takens' theorem [1, 2] which proves that observables measured in any part of a system generically can be used to reconstruct the full state of the overall system. That is, the flow in each reconstruction space uniquely represents the global dynamics, and different reconstructions are therefore topologically equivalent.

For estimating directed dependencies among stochastic variables, Granger Causality [3] is an extensively studied well established method. For dynamical systems, however, applications of Granger Causality for determining influences are conceptually questionable since state reconstructions from different observables of the system contain the identical information about the original state, meaning that the basic premise of separability is violated.

To quantify the strength of mutual influences among parts of dynamical systems, several methods were developed, based on information theory [4, 5] or properties of maps between state space reconstructions from different observables [6, 7]. Recently, Convergent-Cross Mapping [8] was proposed to establish a measure of causal interrelations in dynamical systems, which was shown to yield interesting results in a range of applications (e.g. [8–10]). This procedure proposes certain convergence properties of prediction errors, depending on the number of data points, of one observation from the reconstruction of another as a measure of

causality. However, as noted before, predictability of one component system from another is theoretically always perfect since no information between reconstructions is lost, rendering the method analytically intransparent. Specifically, it does not address the effect of causal interactions on the interrelation of observables directly.

Here we show that causal interactions systematically influence the relation among reconstructions of the state of a dynamical system from two observables. Whereas topology preservation of the mapping from one reconstruction to the other might be used as an all or nothing criterion that would provide a binary measure of causality [11], we discovered that local distortions in this mapping in fact yield continuous values that can be used to determine the causal links among deterministic component systems.

For the intuition behind this idea consider a system composed of two mutually coupled dynamical components 1 and 2, both time continuous deterministic dynamical systems, where the coupling strength  $w_{1 \rightarrow 2}$  (coupling from 1 to 2) is substantial while the other coupling  $w_{2 \rightarrow 1}$  is weak. While according to Takens' Theorem state reconstructions  $r^{x_1}$  from measurements  $x_1$  of system 1, lying in space  $R^{x_1}$ , and reconstructions  $r^{x_2}$  from measurements of system 2, lying in space  $R^{x_2}$ , will both reveal the same global system attractor and are therefore topologically equivalent, the weak coupling from 2 to 1 implies that the homeomorphic map from  $r^{x_1}$  to  $r^{x_2}$ , symbolized by  $M_{1 \rightarrow 2}$ , will provide a 'stretch'. Since we will in practice investigate the mappings locally, this statement translates to the local homeomorphic map  $M_{1 \rightarrow 2}^t$  from a small area around a reference point  $r^{x_1}(t)$  onto  $r^{x_2}$  being stretching for most reference time points  $t$ . This can be visualized as the compound manifold  $(r^{x_1}, r^{x_2})$  lying 'steeply' over  $R^{x_1}$  at most reference points (FIG. 1 A)).

The fact that  $M_{1 \rightarrow 2}$  is the more stretching the weaker the coupling  $w_{2 \rightarrow 1}$  in the *reverse* direction might seem

\* daniel@neuro.uni-bremen.de; <http://neuro.uni-bremen.de>

† pawelzik@neuro.uni-bremen.de; <http://neuro.uni-bremen.de>

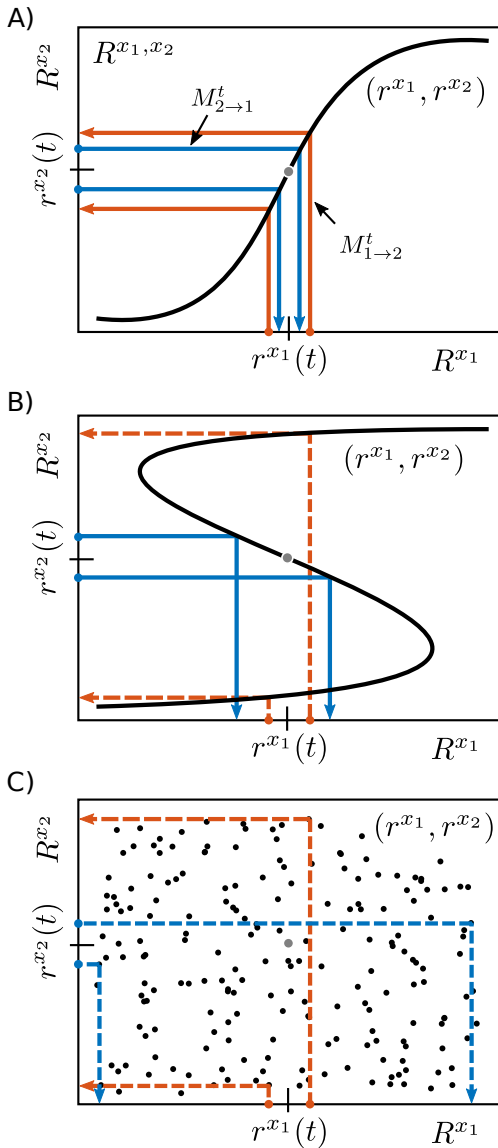


FIG. 1. Illustration of the key idea. A) Larger independence of  $x_1$  implies a stretching by the map  $M_{1 \rightarrow 2}$ . This map can be locally investigated at a reference point  $r^{x_1}(t)$  and is then denoted by  $M_{1 \rightarrow 2}^t$ . While  $R^{x_1}$  and  $R^{x_2}$  are multi-dimensional we can illustrate the stretching only in a one dimensional section of the manifold. It realizes a function  $f: R^{x_1} \rightarrow R^{x_2}$  that has a slope  $> 1$  which in this 1-d representation corresponds to the stretching. B) When the coupling from 1 to 2 vanishes (i.e.  $w_{1 \rightarrow 2} = 0$ ) the situation changes dramatically as compared to A). While there still is a one-to-one mapping  $r^{x_2} \rightarrow r^{x_1}$ , invertibility is lost: not for all states  $r^{x_1}, r^{x_2} \in R^{x_2}$  is uniquely determined. In this case we can attribute the map  $M_{1 \rightarrow 2}$  a diverging stretching property: close neighbours of a given point  $r^{x_1}(t)$  map to distant parts of the density in joint space  $R^{x_1, x_2}$ , i.e. local stretching extends to macroscopic scales. The dashed lines visualize the non-uniqueness of the map. C) If no coupling at all exists, stretching diverges in both directions and nearby points to  $r^{x_1}(t)$  in  $R^{x_1}$  correspond to points  $r^{x_2}$  that are distant from  $r^{x_2}(t)$  in  $R^{x_2}$  and vice versa.

counter intuitive, but it becomes most clear in the limiting case where component system 2 has no influence on 1 (i.e.  $w_{2 \rightarrow 1} = 0$ ). Here Takens' Theorem still holds for reconstructions based on  $x_2$  such that knowledge of the state reconstruction  $r^{x_2}$  fully determines  $r^{x_1}$ . However, reconstructions  $r^{x_1}$  obviously cannot (fully) determine  $r^{x_2}$ , since the latter manifold contains contributions that due to the lack of backward coupling leave not trace in  $r^{x_1}$ . That is, the map  $M_{1 \rightarrow 2}$  loses its uniqueness. This can schematically be illustrated by a manifold  $(r^{x_1}, r^{x_2})$  in the joint space  $R^{x_1, x_2}$  that now lies folded over  $R^{x_1}$ . (FIG. 1 B) illustrates the well defined mapping  $M_{2 \rightarrow 1}$ , while in the inverse direction the mapping  $M_{1 \rightarrow 2}$  does not exist, at least not in the usual sense. In this case we define the stretching from  $r^{x_1}$  to  $r^{x_2}$  to be infinite since it necessarily diverges at the transition  $w_{2 \rightarrow 1} \rightarrow 0$ . Thus, a vanishing coupling  $w_{2 \rightarrow 1}$  entails a divergent stretching from  $r^{x_1}$  to  $r^{x_2}$ .

In practice the local stretching can be obtained by considering close neighbours to a reference point  $r^{x_1}(t)$  in  $R^{x_1}$ . The time points of the  $k$  nearest neighbours to  $r^{x_1}(t)$  shall be given by  $\{q_1^{x_1, t}, \dots, q_k^{x_1, t}\}$ . Then the corresponding points on  $r^{x_2}$ , i.e.  $\{r^{x_2}(q_1^{x_1, t}), \dots, r^{x_2}(q_k^{x_1, t})\}$ , will span the whole dynamical range of  $r^{x_2}$  and thus will not lie in local vicinity to  $r^{x_2}(t)$ .

An even more extreme limit case occurs when both component systems are completely decoupled. Then they will behave independently and the density of the resulting manifold in joint space  $R^{x_1, x_2}$  factorizes. Here, when observed from reference states  $r^{x_1}(t)$  and  $r^{x_2}(t)$ , the mappings can also be considered infinitely stretching, now in both directions, since for most reference points close neighbours in the respective other space are found to be far away (FIG. 1 C)).

Taken together, these topological arguments suggest that the local stretchings of the mappings between reconstruction manifolds of two observables might serve as a viable measure of directed causal influence between component systems represented by these observables.

## TOPOLOGICAL CAUSALITY

The above considerations can be made fully explicit with two coupled time discrete dynamical components for which two-dimensional time-delay coordinates are guaranteed to be sufficient embeddings for the overall dynamics. As a concrete example consider a system of coupled logistic maps described by

$$x_i(t+1) = \left( 1 - \sum_{j \in \{1, \dots, n\} \setminus \{i\}} w_{j \rightarrow i} \right) f_i(x_i(t)) \quad (1)$$

$$+ \sum_{j \in \{1, \dots, n\} \setminus \{i\}} w_{j \rightarrow i} x_j(t)$$

$$f_i(x) \equiv f(x) = 4x(1-x)$$

with  $n = 2$ . Given the reconstruction states  $r^{x_1}(t) = (x_1(t), x_1(t+1))$  and  $r^{x_2}(t) = (x_2(t), x_2(t+1))$ , the local maps  $M_{2 \rightarrow 1}^t$  and  $M_{1 \rightarrow 2}^t$ , which project a small area around the reference point  $r^{x_2}(t)$  onto  $r^{x_1}$  and vice versa, can be calculated. For small perturbations  $\Delta_{x_2} = (\Delta x_2(t), \Delta x_2(t+1))$  around  $r^{x_2}(t)$  one can see that

$$\Delta_{x_1} = \frac{1}{w_{1 \rightarrow 2}} \begin{pmatrix} \hat{f}_2 & 1 \\ w_{2 \rightarrow 1} w_{1 \rightarrow 2} - \hat{f}_1 \hat{f}_2 & -\hat{f}_1 \end{pmatrix} \Delta_{x_2}$$

with

$$\begin{aligned} \hat{f}_2 &= (w_{1 \rightarrow 2} - 1) f'(x_2(t)) \\ \hat{f}_1 &= (w_{2 \rightarrow 1} - 1) f'(x_1(t)) \end{aligned}$$

This linearised perturbation matrix is equal to  $M_{2 \rightarrow 1}^t$  for  $\Delta_{x_2} \rightarrow 0$  and we will use them interchangeably in the following. Equivalently  $M_{1 \rightarrow 2}^t$  can be calculated. The maximal local stretching  $s_{2 \rightarrow 1}^t$  imposed by  $M_{2 \rightarrow 1}^t$  is determined by the eigenvalues of the covariance matrix  $M_{2 \rightarrow 1}^t (M_{2 \rightarrow 1}^t)^T$  in the following way:

$$s_{2 \rightarrow 1}^t = \sqrt{\lambda_{\max}(M_{2 \rightarrow 1}^t (M_{2 \rightarrow 1}^t)^T)}$$

where  $\lambda_{\max}(A)$  is the largest eigenvalue of  $A$ . While the closed form solutions of  $s_{2 \rightarrow 1}^t$  and  $s_{1 \rightarrow 2}^t$  are quite lengthy expressions it can be seen that for small couplings  $w_{1 \rightarrow 2}$ ,  $s_{2 \rightarrow 1}^t$  is dominated by  $1/w_{1 \rightarrow 2}$  and vice versa. This becomes most apparent for  $w_{2 \rightarrow 1} = 0$ , in which case  $s_{2 \rightarrow 1}^t$  simplifies to

$$s_{2 \rightarrow 1}^t = \frac{1}{w_{1 \rightarrow 2}} \sqrt{(w_{1 \rightarrow 2} - 1)^2 f'^2(x_2(t)) + f'^2(x_1(t))} \quad (2)$$

It is obvious that  $\lim_{w_{1 \rightarrow 2} \rightarrow 0} s_{2 \rightarrow 1}^t = \infty$ , confirming the intuition of infinite stretching for vanishing interaction. Additionally, since for small couplings  $w_{1 \rightarrow 2}$ , the stretching is approximated by  $(s_{2 \rightarrow 1}^t)^{-1} \approx w_{1 \rightarrow 2} / \sqrt{f'^2(x_2(t)) + f'^2(x_1(t))}$ , we define a local measure of causality from  $r^{x_1}(t)$  to  $r^{x_2}(t)$  as

$$C_{1 \rightarrow 2}^t := (s_{2 \rightarrow 1}^t)^{-1}$$

This local property for every point on the reconstructed attractors can be turned into a global measure by averaging over the full set of available states:

$$C_{1 \rightarrow 2} := \left( \frac{1}{T} \sum_{t=1}^T s_{2 \rightarrow 1}^t \right)^{-1}$$

This definition, which we term Topological Causality, satisfies the following intuitions about causality: First, causality from component system 1 to 2 vanishes if there is no link via which it can act ( $w_{1 \rightarrow 2} = 0$ ) and secondly, for small couplings it is directly proportional to the coupling strength  $w_{1 \rightarrow 2}$ , at least in

this simple example. However, causality, reflecting the strength of directed influence between the two component systems, is not merely a function of the coupling strength but also depends explicitly on the current state of the systems as well as on the internal dynamics of each component (dependency on  $x_1(t)$ ,  $x_2(t)$  and  $f()$  in Eq. (2)). FIG. 2 A) illustrates the state dependency of  $C_{1 \rightarrow 2}^t$  for a system described by Eqs. (1).

To especially address the asymmetry of causal influences between components 1 and 2, we furthermore define the local asymmetry index  $\alpha_t$  as

$$\alpha_t = \frac{C_{1 \rightarrow 2}^t - C_{2 \rightarrow 1}^t}{C_{1 \rightarrow 2}^t + C_{2 \rightarrow 1}^t}$$

and equivalently for the state-averaged values of  $C$

$$\alpha = \frac{C_{1 \rightarrow 2} - C_{2 \rightarrow 1}}{C_{1 \rightarrow 2} + C_{2 \rightarrow 1}}$$

FIG. 2 B) displays  $\alpha$  for a range of coupling parameters in the model described by Eq. (1), showing that in this example the dominant influence is exerted along the stronger coupling weight. Note however that this is not necessarily the case, e.g. if the internal dynamics of  $x_2$  is generated by a different function  $f_2()$  than the internal dynamics of  $x_1$ .

### Estimating Topological Causality

In cases where the dynamical system model does not allow for an analytical linearisation of the maps between the reconstructed spaces, or the model itself is not known, the stretching by the local maps, and indeed the local maps itself, can be estimated in a purely data-driven manner.

For this, one finds the time indices  $\{q_1^{x_1, t}, \dots, q_k^{x_1, t}\}$  of the  $k$  nearest neighbours on  $r^{x_1}$  around a reference point  $r^{x_1}(t)$ . Now the projection from  $\{r^{x_1}(q_1^{x_1, t}), \dots, r^{x_1}(q_k^{x_1, t})\}$  to  $\{r^{x_2}(q_1^{x_1, t}), \dots, r^{x_2}(q_k^{x_1, t})\}$  is approximately mediated by the linear map  $M_{1 \rightarrow 2}^t$  if the neighbourhood size is sufficiently small compared to the full attractor size. It is then straightforward to estimate  $M_{1 \rightarrow 2}^t$  by solving a simple optimization problem, where in the numerics some care has to be taken when the stretching becomes large. FIG. 2 C) and D) demonstrate that the estimates of  $C^t$ ,  $C$  and  $\alpha$  obtained in this manner are close to the theoretical values for the system given by Eq. (1). A neighbourhood size of  $k = 10$  was used with a total data length of  $T = 10000$ .

### Dynamic Reversals of Causal Asymmetry

Since the influence of a component system onto another may be state dependent, as evident from Eq. (2),

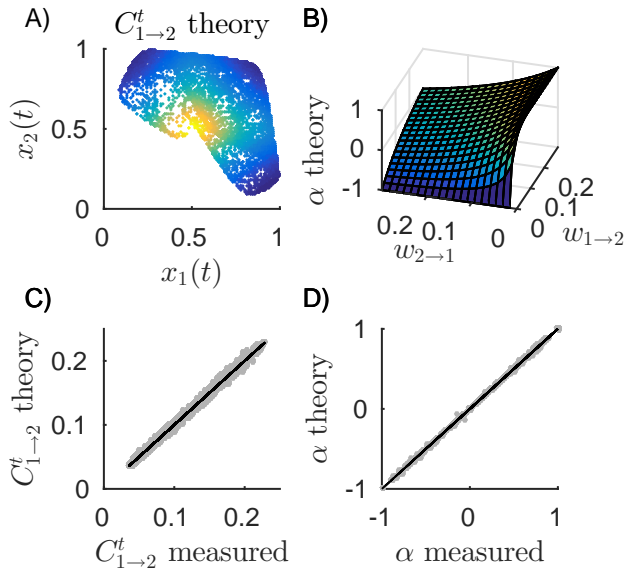


FIG. 2. Topological Causality. A)  $C_{1 \rightarrow 2}^t$  for the system described by equations 1 with  $n = 2$ ,  $w_{1 \rightarrow 2} = 0.3$  and  $w_{2 \rightarrow 1} = 0.23$ . The map was iterated for 10000 time steps and  $C_{1 \rightarrow 2}^t$  and  $C_{2 \rightarrow 1}^t$  calculated analytically at the points the system visited. The state space dependency of  $C_{1 \rightarrow 2}^t$  is clearly visible, where yellow colors correspond to high, green to intermediate and blue ones to low values. B) The asymmetry index  $\alpha$  for a range of coupling parameters in the same model, which accurately reflects the asymmetry in coupling weights such that  $\alpha = 0$  if the coupling weights are equal. C) The theoretical values for  $C_{1 \rightarrow 2}^t$  shown in A) were estimated from the given data alone without knowledge of the underlying model. The gray dots show the point to point comparison and reveal a good agreement of the theoretical and the measured values. D) The theoretical values of  $\alpha$  in B) are compared with the measured values, and again a good agreement is found.

so can the asymmetry index  $\alpha_t$ . This phenomenon can be investigated in coupled time-discrete maps that are non-linearly coupled. As an example consider the system given by

$$\begin{aligned} x_1(t+1) &= x_1(t)(3.8(1-x_1(t)) - w_{2 \rightarrow 1}x_2(t)) \\ x_2(t+1) &= x_2(t)(3.8(1-x_2(t)) - w_{1 \rightarrow 2}x_1(t)) \end{aligned} \quad (3)$$

Also in this case the maps  $M_{1 \rightarrow 2}^t$  and  $M_{2 \rightarrow 1}^t$  can be calculated analytically and for weak coupling weights  $w$  it turns out that  $s_{1 \rightarrow 2}^t \propto 1/(x_1(t)w_{2 \rightarrow 1})$  and  $s_{2 \rightarrow 1}^t \propto 1/(x_2(t)w_{1 \rightarrow 2})$ . Thus, the map  $M_{1 \rightarrow 2}^t$  is extremely steep for low  $x_1$  values, and the map  $M_{2 \rightarrow 1}^t$  for low values of  $x_2$ . Consequently, as shown in FIG. 3 A) and B), although the coupling weights do not change over time, the asymmetry index  $\alpha_t$  fluctuates considerably as the system explores the attractor. FIG. 3 C) illustrates how this change of causal dominance over time gives rise to various dynamical regimes among the time courses of  $x_1$  and  $x_2$ .

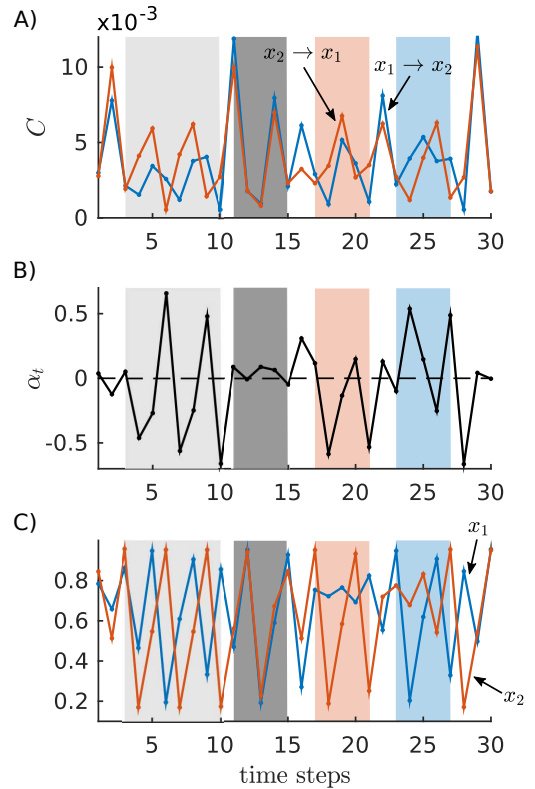


FIG. 3. State dependency of causal influences. A) shows the change over time of  $C_{1 \rightarrow 2}^t$  and  $C_{2 \rightarrow 1}^t$  in a system governed by Eqs. (3) with  $w_{1 \rightarrow 2} = w_{2 \rightarrow 1} = 0.024$ . B) Consequently the asymmetry index  $\alpha_t$  shows a time dependency as well. Several regions are highlighted in different colors: A region in which the mean over time of  $\alpha_t$  is close to 0 and the variance is high (light gray), one with similar mean but low variance (dark gray), one in which the mean is  $< 0$  (orange), indicating stronger influence  $2 \rightarrow 1$  than vice versa, and one in which the mean is  $> 0$  (blue), indicating stronger influence  $1 \rightarrow 2$  than vice versa. The same regions are marked accordingly in C) and A). C) original time series of  $x_1$  and  $x_2$ . The different regimes of causal asymmetry, marked by the shadings, give rise to different dynamical motifs. If  $\alpha_t$  varies strongly around 0 (light gray),  $x_1$  and  $x_2$  desynchronize. If  $\alpha_t$  is close to 0 for subsequent time points (dark gray),  $x_1$  and  $x_2$  synchronize. When the causal influence is stronger from  $2 \rightarrow 1$  than vice versa (orange),  $x_2$  is more independent while movement of  $x_1$  is constrained. The reverse is seen when the influence  $1 \rightarrow 2$  is dominant (blue).

### Divergence, Transitivity and Convergence

In order to serve as a satisfactory definition of causality in dynamical systems, Topological Causality must obey fundamental requirements that can be demonstrated by examining simple network motifs.

The first prerequisite is the ability to distinguish shared input from true interaction. Consider a system described by Eqs. (1) with  $n = 3$ , where only  $w_{3 \rightarrow 1} \neq 0$  and  $w_{3 \rightarrow 2} \neq 0$ , generating a divergent network motif.

With moderate coupling from  $x_3$  to  $x_1$  and  $x_2$ , the latter two do not become fully enslaved and, in particular, do not synchronize (which otherwise would represent an irrelevant singular case). Still the usual Pearson Correlation Coefficient (*PCC*) can reach substantial values which obviously do not represent the total absence of causal links among  $x_1$  and  $x_2$ . In contradistinction, the proposed method yields values for the causal couplings that are low and relatively independent of the common drive, reflecting the actual causal influences (FIG. 4 A)). Intuitively this result is easily understood: in the respective reconstruction spaces the independent dynamics of the component systems explore independent directions which induces diverging stretching of the mappings among the respective manifolds. This results demonstrates that in dynamical systems Topological Causality can indeed separate causal links from common causes.

The second required property is transitivity, meaning that 'if 1 causes 2 and 2 causes 3, then 1 causes 3'. Since  $M_{3 \rightarrow 1}^t = M_{2 \rightarrow 1}^t M_{3 \rightarrow 2}^t$ , it can be shown by simple algebraic manipulation that

$$\begin{aligned} C_{1 \rightarrow 3}^t &> C_{1 \rightarrow 2}^t C_{2 \rightarrow 3}^t && \text{if } w_{1 \rightarrow 2} \neq 0 \wedge w_{2 \rightarrow 3} \neq 0 \\ C_{1 \rightarrow 3}^t &= 0 && \text{else} \end{aligned}$$

meaning that transitivity is mathematically guaranteed. We illustrate this numerically in FIG. 4 B) for a system modelled by Eqs. (1), with  $n = 3$  and where  $w_{1 \rightarrow 2}$  and  $w_{2 \rightarrow 3}$  are the only existing links.

In addition, the measure should be able to deal with convergent influences. Unfortunately, if a network of three coupled maps given by Eqs. (1) has a convergent motif such that  $x_1$  and  $x_2$  are independently influencing  $x_3$ , a sufficient embedding is not possible with a low number of delay coordinates. Therefore, convergence needs to be investigated with time continuous component systems for which Takens' Theorem is guaranteed to hold. For this we use three coupled sets of Lorenz equations:

$$\dot{x}_i(t) = 10 \left( y_i(t) - \left( x_i(t) - \sum_{j \in \{1,2,3\} \setminus \{i\}} w_{j \rightarrow i} x_j(t) \right) \right) \quad (4)$$

$$\dot{y}_i(t) = x_i(t)(28 - z_i(t)) - y_i(t)$$

$$\dot{z}_i(t) = x_i(t)y_i(t) - \frac{8}{3}z_i(t)$$

A convergence motif is achieved when only the coupling weights  $w_{1 \rightarrow 3}$  and  $w_{2 \rightarrow 3}$  are nonzero. FIG. 4 C) shows that the causal influence of the driving component system with the stronger link to the receiving component system is consistently higher than the influence from the other, which is expected for three coupled systems whose internal dynamics are governed by the same model.

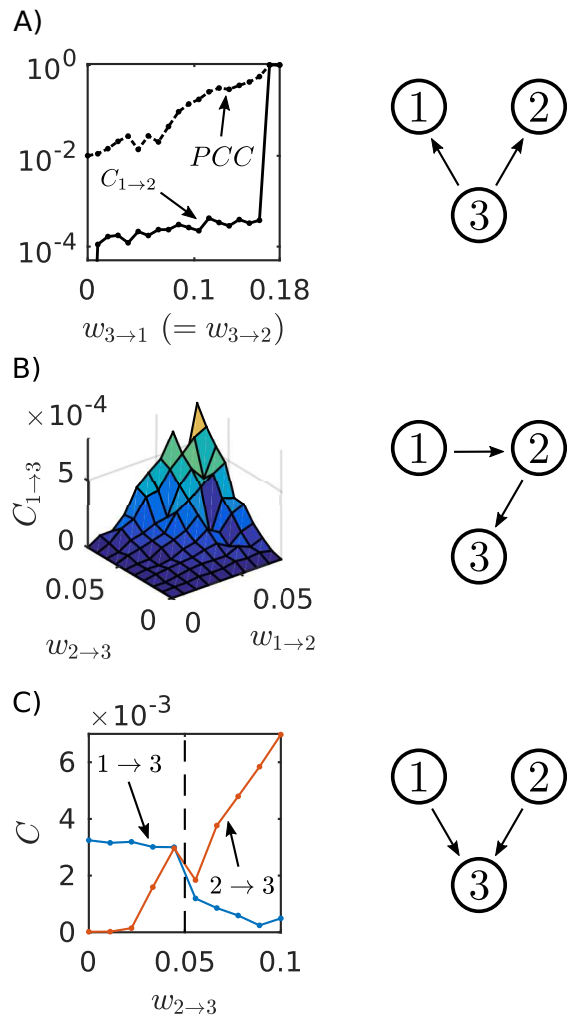


FIG. 4. Fundamental properties of Topological Causality. A) Common input (divergence motif). The plot shows  $C_{1 \rightarrow 2}$  in a system described by Eqs. (1) with  $n = 3$  and  $w_{1 \rightarrow 2} = w_{2 \rightarrow 1} = 0$  along with the Pearson Correlation Coefficient (*PCC*) between  $x_1$  and  $x_2$  when a third dynamical variable  $x_3$  is fed into both  $x_1$  and  $x_2$  with equal weight  $w_{3 \rightarrow 1} = w_{3 \rightarrow 2}$ .  $C_{1 \rightarrow 2}$ , and  $C_{2 \rightarrow 1}$  (not shown) depend only weakly on the common input unless the correlation approaches 1, in which case  $x_1$  and  $x_2$  become redundant. B) Same system as in A), but now only  $w_{1 \rightarrow 2} \neq 0$  and  $w_{2 \rightarrow 3} \neq 0$ , giving a unidirectionally coupled chain  $x_1 \rightarrow x_2 \rightarrow x_3$ . One observes  $C_{1 \rightarrow 3} > 0$  if both  $w_{1 \rightarrow 2} > 0$  and  $w_{2 \rightarrow 3} > 0$ , showing the basic property of transitivity. C) The case of convergence is given when dynamical component system 1 and 2 act independently on 3 and no other links exist. The dynamical components are Lorenz systems described by Eqs. (4), where only  $w_{1 \rightarrow 2}$  and  $w_{2 \rightarrow 3}$  are nonzero. For  $w_{1 \rightarrow 2} = 0.05$  and varying  $w_{2 \rightarrow 3}$ , the system with the stronger link to 3 has a higher causal influence  $C$ . The chosen embedding dimension here is 19, and the local maps were estimated with  $k = 400$  and a full time series length of  $T = 1000k$ .

### Noise Robustness

Lastly, we address the question of noise robustness. We investigate the noise dependency of the asymmetry index  $\alpha$  for two coupled Lorenz systems described by Eqs. (4) with  $n = 2$ . FIG. 5 shows  $\alpha$  for various combinations of  $w_{1 \rightarrow 2}$  and  $w_{2 \rightarrow 1}$  in a noise-free case and for 5% and 10% of additive Gaussian noise. Whereas the numerical values for the noiseless case are not faithfully reproduced, the directionality given by the sign of  $\alpha$  is consistent and especially the case when  $w_{1 \rightarrow 2} = 0$  is correctly captured by a value of  $\alpha \approx -1$ .

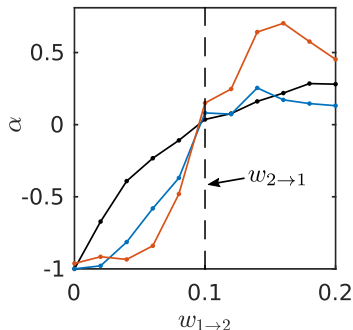


FIG. 5. Noise robustness. The values of  $\alpha$  are shown for two coupled Lorenz-systems described by Eqs. (4) with a fixed coupling  $w_{2 \rightarrow 1} = 0.1$  and a range of different values for  $w_{1 \rightarrow 2}$ . The embedding dimension was chosen as 13,  $k = 200$  and  $T = 1000 - k$ . The black line displays the result in the noiseless case which serves as a benchmark since the analytical result is not accessible for this system. The two estimates under conditions of additive Gaussian noise (5%: blue line; 10%: orange line) still succeed in capturing the sign of the asymmetry.

### DISCUSSION

For the analysis of complex systems like the brain, the economy, the climate or the biosphere it is of huge interest to identify causal links among their components. Here, a definition of causality was proposed, termed Topological Causality, that provides an estimate of the sizes and, in particular, of the dominant direction of effective influence among parts of a dynamical system represented by observables of interest. The definition follows heuristic considerations of influence-induced distortions in the mappings between state space reconstructions of component variables.

It was shown that this 'Topological Causality' fulfills basic requirements that a measure of causality must obey, such as disentanglement of causal influence from common input and transitivity.

A prominent concept implied by the current definition is that the effective influence of one part of a system depends on the state of the whole system, meaning that in

general Topological Causality is related but not identical to coupling. The latter entails the possibility of temporal variations of the mutual effective influences, which indeed can be captured by the proposed method.

The current work is related to the procedure of Convergent Cross-Mapping (CCM), introduced by [8] to overcome the limitations of Granger Causality [3]. CCM exploits the 'difficulty' of predicting one attractor reconstruction from another (i.e. the convergence time) as an indirect measure of the strength of causal influence. We hypothesize that this difficulty of prediction is a direct consequence of the stretching of the mapping, which Topological Causality measures directly: It seems reasonable that if a mapping between reconstructions is more stretching, the error of prediction in direction of this mapping tends to be larger, thus convergence of prediction error tends to be slower. A recent extension of the CCM method investigates the 'smoothness' of maps between reconstructions [12], a concept reminiscent of the Wavering Product [11], which was introduced to detect violations of topological equivalence. But, whereas the smoothness of a map correlates to the stretching in a way that a strongly stretching, non-topology-preserving map will also be not smooth, an interpretation of the various levels of smoothness in terms of effective interactions among component systems is difficult.

While the notion of causality is problematic due to the known generic lack of separability of mutually coupled dynamical component systems, the definition of Topological Causality we put forward here allows for a surprisingly clear mathematical interpretation: in simple cases it was found to be fully analytically tractable and reflects the directed effective influences including their state (and time) dependence. The demonstrated robustness of this measure to noise added to observables from model systems holds promise that Topological Causality will yield useful results also when applied to real data which, however, remains to be explored.

### ACKNOWLEDGMENTS

DH was funded by the Bundesministerium für Bildung und Forschung (Bernstein Award Udo Ernst, Grant 01GQ1106) and thanks Dr. Udo Ernst for support during the project.

- 
- [1] N. H. Packard, J. P. Crutchfield, J. D. Farmer, and R. S. Shaw, *Phys. Rev. Lett.* **45**, 712 (1980).
- [2] F. Takens, in *Dynamical Systems and Turbulence*, Springer Lecture Notes in Mathematics, Vol. 898, edited by D. A. Rand and L.-S. Young (Springer-Verlag, Berlin, 1981).
- [3] C. W. J. Granger, *Econometrica* **37**, 424 (1969).
- [4] T. Schreiber, *Phys. Rev. Lett.* **85**, 461 (2000).
- [5] M. Paluš, V. Komárek, Z. Hrnčíř, and K. Štěrbová, *Phys. Rev. E* **63**, 046211 (2001).
- [6] S. J. Schiff, P. So, T. Chang, R. E. Burke, and T. Sauer, *Phys. Rev. E* **54**, 6708 (1996).
- [7] D. Chicharro and R. G. Andrzejak, *Phys. Rev. E* **80**, 026217 (2009).
- [8] G. Sugihara, R. M. May, H. Ye, C. Hsieh, E. R. Deyle, and M. Fogarty, *Science* **334**, 496 (2012).
- [9] X. Wang, S. Piao, P. Ciais, P. Friedlingstein, R. B. Myneni, P. Cox, M. Heimann, J. Miller, S. Peng, T. Wang, H. Yanga, and A. Chen, *Nature* **506**, 212 (2014).
- [10] S. Tajima, T. Yanagawa, N. Fujii, and T. Toyozumi, *PLoS Comp. Biol.* **1004537** (2015).
- [11] W. Liebert, K. R. Pawelzik, and H. G. Schuster, *Europhysics Letters* **14**, 521 (1991).
- [12] H. Ma, K. Aihara, and L. Chen, *Scientific Reports* **4**, 7464 (2014).